Basolateral amygdala input to the medial prefrontal cortex controls obsessive-compulsive disorder-like checking behavior

Tingting Sun[a,1], Zihua Song[a,1], Yanghua Tian[b,1], Wenbo Tian[a], Chunyan Zhu[b], Gongjun Ji[b], Yudan Luo[b], Shi Chen[c], Likui Wang[c], Yu Mao[a,d], Wen Xie[e], Hui Zhong[e], Fei Zhao[f], Min-Hua Luo[f], Wenjuan Tao[a], Haitao Wang[a], Jie Li[a], Juan Li[a], Jiangning Zhou[a], Kai Wang[b,2], and Zhi Zhang[a,2]

[a]Hefei National Laboratory for Physical Sciences at the Microscale, Department of Biophysics and Neurobiology, University of Science and Technology of China, Hefei, Anhui 230027, People's Republic of China; [b]Department of Neurology, The First Affiliated Hospital of Anhui Medical University, Hefei, Anhui 230022, People's Republic of China; [c]Department of Pain Management, The First Affiliated Hospital of Anhui Medical University, Hefei, Anhui 230022, People's Republic of China; [d]Department of Anesthesiology, The First Affiliated Hospital of Anhui Medical University, Hefei, Anhui 230022, People's Republic of China; [e]Department of Psychology, Anhui Mental Health Center, Hefei, Anhui 230026, People's Republic of China; and [f]State Key Laboratory of Virology, Chinese Academy of Sciences Center for Excellence in Brain Science and Intelligence Technology, Wuhan Institute of Virology, Chinese Academy of Sciences, Wuhan 430071, People's Republic of China

Edited by Solomon H. Snyder, Johns Hopkins University School of Medicine, Baltimore, MD, and approved January 9, 2019 (received for review August 24, 2018)

Obsessive-compulsive disorder (OCD) affects ∼1 to 3% of the world's population. However, the neural mechanisms underlying the excessive checking symptoms in OCD are not fully understood. Using viral neuronal tracing in mice, we found that glutamatergic neurons from the basolateral amygdala (BLA^{Glu}) project onto both medial prefrontal cortex glutamate ($mPFC^{Glu}$) and GABA ($mPFC^{GABA}$) neurons that locally innervate $mPFC^{Glu}$ neurons. Next, we developed an OCD checking mouse model with quinpirole-induced repetitive checking behaviors. This model demonstrated decreased glutamatergic mPFC microcircuit activity regulated by enhanced BLA^{Glu} inputs. Optical or chemogenetic manipulations of this maladaptive circuitry restored the behavioral response. These findings were verified in a mouse functional magnetic resonance imaging (fMRI) study, in which the BLA–mPFC functional connectivity was increased in OCD mice. Together, these findings define a unique BLA^{Glu}→$mPFC^{GABA→Glu}$ circuit that controls the checking symptoms of OCD.

OCD checking symptoms | neural circuit | BLA | mPFC

Obsessive-compulsive disorder (OCD) is a common and debilitating neuropsychiatric disorder characterized by persistent intrusive thoughts (obsessions) and repetitive actions (compulsions) (1–3). The etiology and pathology of OCD remain poorly understood, making therapy challenging for clinicians (4).

Dysfunction of the cortico-striato-thalamo-cortical (CSTC) circuits, including serotonin, dopamine, and glutamate systems, is thought to underlie certain types of OCD symptoms (5–9). However, a single model is insufficient to clarify OCD pathophysiology, because different OCD symptom dimensions (e.g., symmetry/ordering vs. contamination/washing) may have different underlying neural substrates (10). For example, the CSTC circuits have been proposed to mediate fear of contamination in OCD, while discrete circuits in the insular cortex have been elucidated as the primary loci of symptom generation (11). Notably, pharmacological options for the treatment of OCD remain fairly limited. Selective serotonin reuptake inhibitors are the first-line drugs for the treatment of OCD, but 40 to 60% of patients respond poorly to this treatment (4). This suggests that integration of other brain structures beyond the CSTC circuits may be required to establish causal links in OCD pathophysiology (12).

Preliminary findings with glutamatergic neurotransmission-modulating agents have been promising for the treatment of OCD (13, 14). However, it has not been clear whether defects in the glutamatergic system are primary cause and how the precise glutamate circuits beyond segregated CSTC pathways encode OCD symptoms such as compulsive checking. Therefore, we targeted the glutamate projecting system to identify the precise circuit and to examine its function in compulsive checking behavior.

The amygdaloid complex, which is composed of the basolateral amygdala (BLA), lateral amygdala, and central amygdala, is known for its relevance to fear, anxiety, and reward (15, 16). Imaging studies have shown significant alterations in the volume and activity of the amygdala in OCD patients (17). Even the brain regions in the CSTC pathways have been reported to interact with the amygdala in processing cognition and emotion (18). For example, the reciprocal glutamatergic connections between the BLA and the medial prefrontal cortex (mPFC) have been highly implicated in fear acquisition, expression, and extinction (19, 20). This raises the possibility that the amygdala—in particular the BLA, which consists of ∼90% glutamatergic neurons (21)—could be an important site for processing OCD checking symptoms. Based on the evidence linking the amygdala and CSTC brain regions with emotional regulation, here we addressed the pathological causes of the OCD checking symptoms

Significance

The pathophysiology underlying obsessive-compulsive disorder (OCD) remains unclear, leading to major challenges in the treatment of OCD patients. Here, we defined a projection from the basolateral amygdala glutamate neurons to the medial prefrontal cortex glutamate and GABA neurons and described the putative importance of this circuit in manifesting the checking symptoms of OCD in mice. In addition, the above major findings were further verified in an fMRI mouse study. These findings raise the possibility of developing optimal treatments for OCD that involve the use of nondrug approaches, such as transcranial magnetic stimulation, that target the converging pathways.

Author contributions: K.W. and Z.Z. designed research; T.S., Z.S., Y.T., and W. Tian performed research; C.Z., G.J., S.C., L.W., Y.M., W.X., H.Z., F.Z., M.-H.L., W. Tao, H.W., Jie Li, Juan Li, J.Z., and Z.Z. contributed new reagents/analytic tools; T.S. and Y.L. analyzed data; and T.S. and Z.Z. wrote the paper.

The authors declare no conflict of interest.

This article is a PNAS Direct Submission.

[1]T.S., Z.S., and Y.T. contributed equally to this work.

[2]To whom correspondence may be addressed. Email: wangkai1964@126.com or zhizhang@ustc.edu.cn.

This article contains supporting information online at www.pnas.org/lookup/suppl/doi:10.1073/pnas.1814292116/-/DCSupplemental.

Published online February 11, 2019.

by defining the precise BLA circuits through which excessive checking states are orchestrated by glutamate under OCD conditions.

Results

A Mouse Model of Checking Behavior. To identify the neural circuitry controlling OCD checking behaviors, it is necessary to consider behavior in animals that resembles the checking symptoms of OCD patients. Given that rats treated with the dopamine agonist quinpirole develop checking behavior, we developed a convenient mouse model of OCD-like checking behavior in favor of optogenetic manipulation (22–24). To explore mouse behavior after chronic quinpirole treatment, we designed an experimental setup in which mice received 10% sucrose solution and water (Fig. 1 *A* and *B*). Compared with saline-treated mice, the quinpirole-treated mice rapidly exhibited repetitive checking behaviors, revisiting the home base and container of sucrose more excessively than any other place after 30 d of training. The frequency and the total time of sucrose solution drinking were increased (Fig. 1 *C* and *D*), while the consumption of sucrose solution did not change (*SI Appendix*, Fig. S1*A*). Furthermore, the quinpirole mice displayed anxietylike behaviors in open-field testing, compared with the control group (*SI Appendix*, Fig. S1*B*). Notably, these behavioral characteristics lasted for 21 d after quinpirole withdrawal (*SI Appendix*, Fig. S1 *C* and *D*), which is much longer than the duration observed in quinpirole-treated rats (22, 23). Of note, upon chronic quinpirole treatment without the environmental training with sucrose and an opaque home base in the mouse cage, the mice displayed no repetitive checking behavior (*SI Appendix*, Fig. S1 *E* and *F*).

To rule out the possibility that the compulsive drinking behavior was due to sucrose preference, we exchanged the positions of sucrose and water (Fig. 1*E*). Strikingly, the frequency and time of drinking water, but not sucrose, increased in the quinpirole mice (Fig. 1 *F* and *G*). These findings suggest that the mice followed a rigid route as well as checking behavior accompanied by anxiety, which are prominent features in OCD checkers (10).

To search the specific brain regions involved in the development of OCD-like checking behavior, we investigated the expression of c-Fos protein in the brain after 30 d of drinking training (25). Compared with saline-treated mice, drinking training induced massive c-Fos expression in the mPFC, BLA, and primary somatosensory cortex of quinpirole mice (Fig. 1 *H* and *I* and *SI Appendix*, Fig. S2). In contrast, these differences were not observed on days 6, 10, and 14 after quinpirole treatment (*SI Appendix*, Fig. S3), and the mice had no repetitive checking behavior at these time points (Fig. 1 *C* and *D*).

Because altered volume and activation have been reported in the amygdala of OCD patients (17), we set out to target the amygdala-projecting system to verify the changes in OCD mice. Using resting-state fMRI, we found significant perturbations in the brain functional connectivity of BLA–mPFC in OCD mice compared with controls (*SI Appendix*, Fig. S4). To the best of our knowledge, there have been no previous reports in mice describing the BLA–mPFC pathway in the process of OCD checking symptoms (26, 27). We next focused on the role of this pathway in OCD-like checking symptoms.

The BLA^{Glu} Projects onto mPFC Neurons. A retrograde trans-monosynaptic tracing system was employed to characterize the BLA–mPFC contacts. *Cre*-dependent adeno-associated helper viruses (AAV-Ef1α-DIO-TVA-GFP and AAV-Ef1α-DIO-RVG) were injected into the mPFC of Ca^{2+}/*calmodulin-dependent protein kinase II* (*CaMKII*, an enzyme in glutamatergic neurons)-*Cre* mice and *glutamic acid decarboxylase 2* (*GAD2*, a GABA-synthesizing enzyme)-*Cre* mice. After 3 wk, rabies virus (RV) (EnvA-pseudotyped RV-ΔG-DsRed) was injected into the same site (Fig. 2*A*). The presence of these helper viruses enabled the RV to spread to monosynapses retrogradely (28). In addition to the well-characterized mPFC inputs, such as the ventral hippocampus and the thalamus (*SI Appendix*, Fig. S5), we found intensely DsRed-labeled neurons in the BLA (Fig. 2 *B* and *C*). Quantification showed that the BLA projected preferentially onto GABAergic neurons in the mPFC (Fig. 2*D*). Moreover, the DsRed signal was colocalized with the glutamate antibody based on immunofluorescence staining (Fig. 2*E*). These results indicate that both mPFC glutamatergic ($mPFC^{Glu}$) and GABAergic ($mPFC^{GABA}$) neurons receive BLA glutamatergic (BLA^{Glu}) neuron projections.

To characterize the functional connections within the BLA–mPFC pathway, *Cre*-dependent channelrhodopsin-2 (AAV-DIO-ChR2-mCherry) virus was infused into the BLA of *CaMKII-Cre*

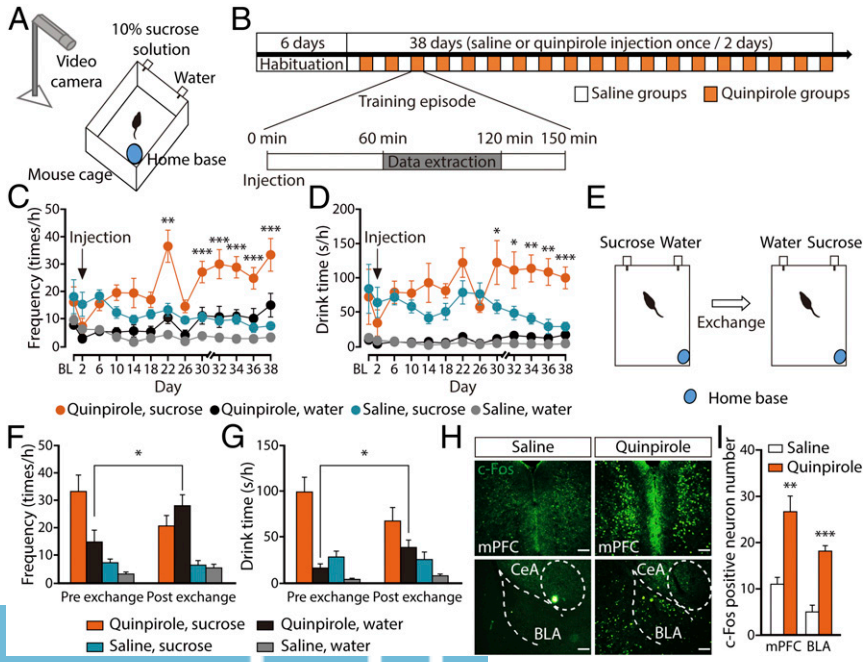

Fig. 1. Mouse model of OCD-like checking behavior. (*A*) Diagram of drinking behavior. (*B*) Timeline for training paradigm. (*C* and *D*) Frequency and duration of sucrose/water drinking of mice treated with quinpirole or saline [$n = 7$ to 9 mice per group, (saline, sucrose) vs. (quinpirole, sucrose), frequency: $F_{1,14} = 18.39$, $P < 0.001$; drink time: $F_{1,14} = 8.96$, $P = 0.0097$]. (*E*–*G*) After exchanging the positions of sucrose solution and water (*E*), the frequency (*F*) and duration of water drinking (*G*) were increased in quinpirole mice relative to saline mice on day 39 ($n = 7$ to 9 mice per group, frequency: $t_6 = -3.41$, $P = 0.014$; drink time: $t_6 = -3.11$, $P = 0.021$). (*H* and *I*) Distribution of c-Fos–positive neurons in the mPFC and BLA in mice treated with quinpirole or saline ($n = 5$ to 7 slices from three mice per group, mPFC: $t_{12} = -4.31$, $P = 0.001$; BLA: $t_9 = -7.08$, $P < 0.001$). Average c-Fos–positive neurons per 0.04 mm^2 imaging area. (Scale bars: 50 μm.) Data are means ± SEM. $^*P < 0.05$, $^{**}P < 0.01$, $^{***}P < 0.001$. Two-way repeated-measures ANOVA with Bonferroni post hoc analysis for *C* and *D*; paired *t* test for *F* and *G*; unpaired *t* test for *I*.

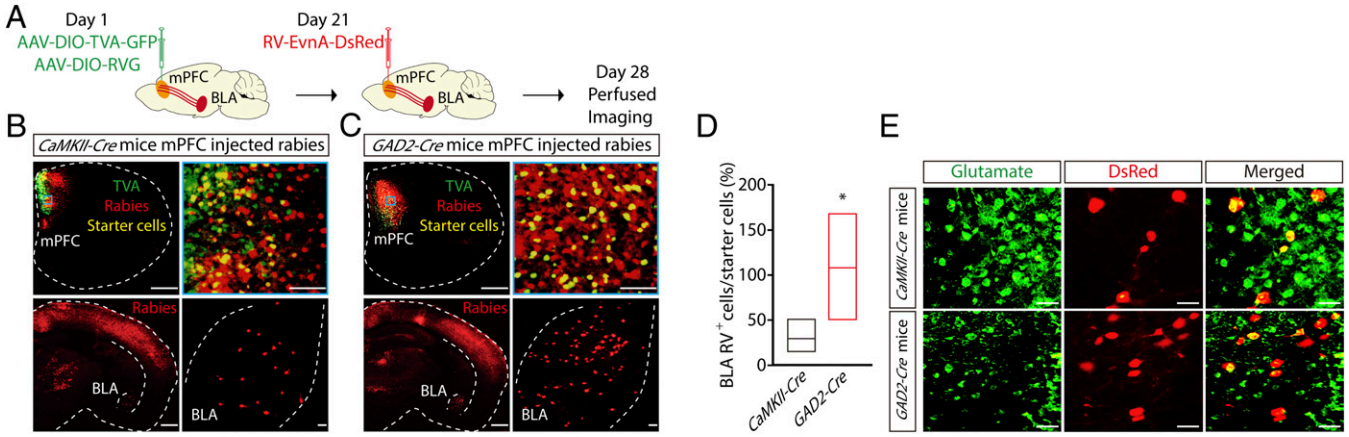

Fig. 2. BLA^{Glu} neurons preferentially synapse on mPFC^{GABA}. (*A*) Schematic of the retrograde transmonosynaptic RV tracing strategy. (*B* and *C*, *Top*) Typical images of injection sites and viral expression within the mPFC of *CaMKII-Cre* (*B*) and *GAD2-Cre* (*C*) mice. Starter cells (yellow) coexpressing AAV-DIO-TVA-GFP, AAV-DIO-RVG (green), and RV-EnvA-ΔG-DsRed (red). The blue boxes in the *Left* images depict the area shown in the *Right* boxes. (*B* and *C*, *Bottom*) DsRed-labeled neurons within the BLA traced from the mPFC. [Scale bars: 500 μm (*Left*), 50 μm (*Right*).] (*D*) Quantification of DsRed (RV)-labeled cells in the BLA (n = 3 to 5 slices from four mice per group, $t_6 = -3.03$, $P = 0.023$). (*E*) DsRed signals were colocalized with the glutamate immunofluorescence in the BLA. (Scale bars: 25 μm.) Data are means ± SEM. *$P < 0.05$. Unpaired t test for *D*.

mice (Fig. 3*A*). We observed mCherry$^+$ (glutamate) cell bodies in the BLA and numerous mCherry$^+$ fibers in the mPFC (Fig. 3*B*). At −70 mV holding potential, optical stimulation of ChR2-containing BLA^{Glu} terminals in the mPFC reliably elicited excitatory postsynaptic currents (EPSCs) in mPFC^{Glu} neurons, which were blocked by the AMPA receptor antagonist 6,7-dinitroquinoxaline-2,3-dione in brain slices (Fig. 3 *C* and *D*). At 0 mV holding potential, inhibitory postsynaptic currents (IPSCs) were elicited in the same neurons by photostimulation and were eliminated by the $GABA_A$ receptor antagonist bicuculline (Fig. 3 *E*–*G*). Notably, the latency to light-evoked EPSCs was lower than that to IPSCs. In addition, EPSCs were also induced in mPFC^{GABA} neurons by photostimulation (Fig. 3*H*). These results reveal a microcircuit organization wherein mPFC^{Glu} neurons are innervated by local mPFC^{GABA} interneurons, both of which receive direct BLA^{Glu} inputs (Fig. 3*I*). Light stimulation of mPFC^{GABA} neurons elicited IPSCs in local glutamate neurons in *GAD2-Cre* mice by mPFC injection of AAV-DIO-ChR2-mCherry, confirming this hypothesis (*SI Appendix*, Fig. S6).

Increased Excitability of mPFC-Projecting BLA^{Glu} Neurons Controls OCD-Like Checking Behavior. To determine the activity of mPFC-projecting BLA^{Glu} neurons in OCD, whole-cell recordings were performed in brain slices from mice with mPFC infusion of the retrograde tracer Fluoro-Gold (FG) (Fig. 4*A*). We observed that BLA FG$^+$ neurons were mostly glutamatergic (87.57 ± 0.028%, Fig. 4 *B* and *C*), consistent with reports that the BLA consists of 90% glutamatergic neurons (21). In response to a series of current injections, we found an increase in the spike number of BLA FG$^+$ neurons from quinpirole mice compared with those

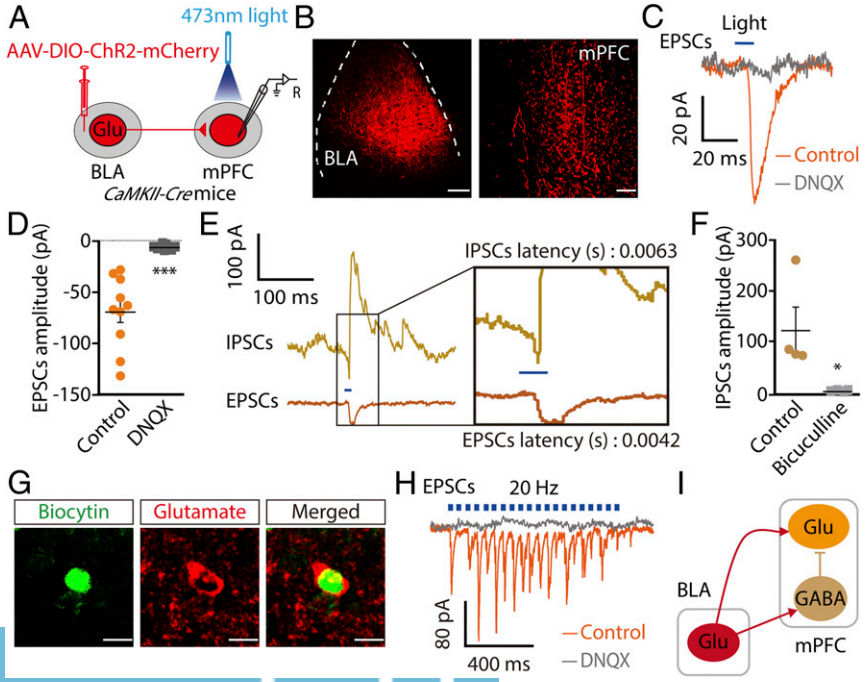

Fig. 3. Synaptic connectivity of the BLA^{Glu}→mPFC$^{GABA→Glu}$ circuit. (*A*) Schematic of viral injection and whole-cell recording in brain slices. (*B*) Representative images of the injection sites and viral expression in the BLA (*Left*) and mPFC (*Right*). (Scale bars: 50 μm.) (*C*) EPSCs were recorded at −70 mV from an mPFC neuron after photostimulation of BLA^{Glu} fibers before and after bath application of 10 μM 6,7-dinitroquinoxaline-2,3-dione (DNQX). (*D*) Summarized data of the light-evoked EPSC amplitude (n = 10 neurons, $t_9 = -5.77$, $P = 0.0003$). (*E*) Typical current traces recorded from the same mPFC neuron after photostimulation of BLA^{Glu} fibers. The box in the *Left* image depicts the area shown in the *Right* image. (*F*) Summarized data showing the amplitude of light-evoked IPSCs before and after bath application of 10 μM bicuculline (n = 4 neurons, $t_3 = 2.54$, $P = 0.042$). (*G*) Recording of an mPFC neuron filled with biocytin showing glutamate. (Scale bars: 10 μm.) (*H*) EPSCs recorded from an mPFC^{GABA} neuron after photostimulation (20 Hz) of BLA^{Glu} fibers before and after bath application of 10 μM DNQX. (*I*) Schematic illustration of BLA^{Glu} projections onto mPFC neurons. Data are means ± SEM. *$P < 0.05$, ***$P < 0.001$. Paired t test for *D* and *F*.

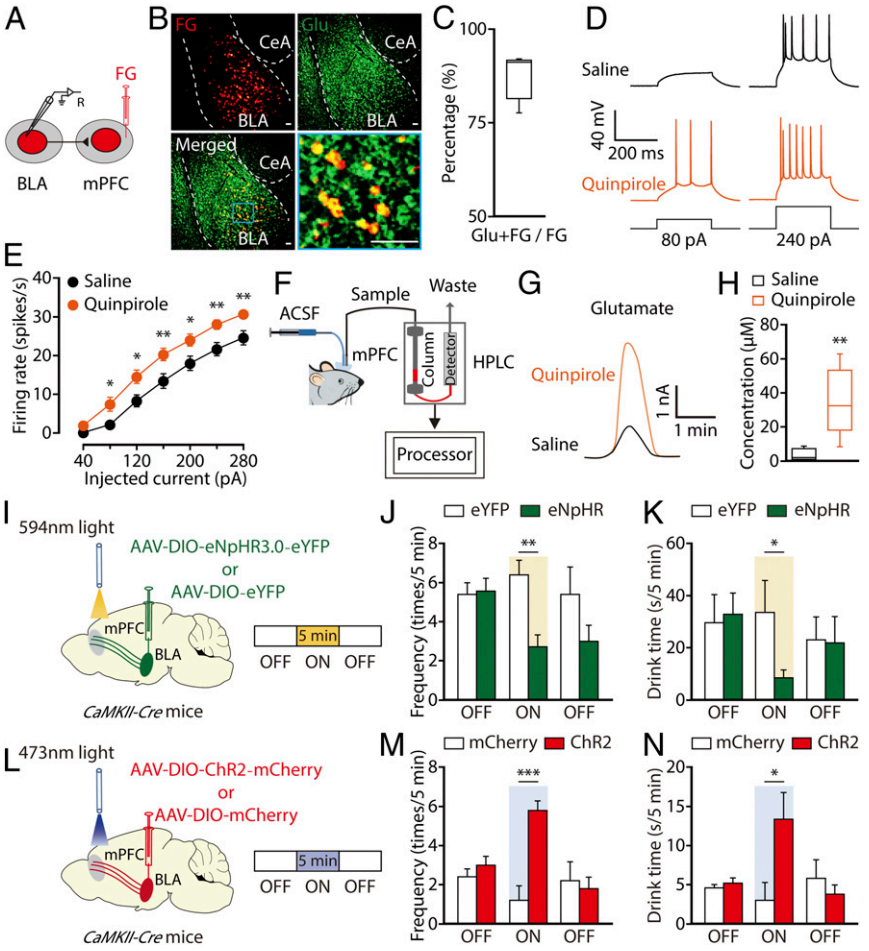

Fig. 4. Increased excitability of mPFC-projecting BLA^{Glu} neurons controls OCD-like checking behavior. (*A*) Schematic diagram for FG injection and whole-cell recording in brain slices. (*B*) Example images of FG-positive neurons (red) merged with the glutamate-positive neurons (green) in the BLA. (Scale bars: 50 μm.) (*C*) Percentage of FG-labeled neurons that expressed glutamate in the BLA (n = 5 slices from three mice). (*D*) Representative traces of voltage responses recorded from FG$^+$ BLA neurons in slices from mice treated with quinpirole or saline for 30 d. (*E*) Summarized data showing firing rates of evoked action potentials in the groups as indicated in *D* (n = 18 neurons per group, $F_{1,34}$ = 9.19, P = 0.005). (*F*) Schematic of microdialysis-HPLC detection in freely moving mice. (*G*) Representative traces of glutamate signals from the mPFC. (*H*) Summarized data showing glutamate concentrations in the mPFC of mice treated with quinpirole or saline for 30 d (n = 5 mice per group, t_8 = –3.44, P = 0.009). (*I*) Schematic of viral injection and the optical configuration in vivo. (*J* and *K*) OCD-like behavioral effects of optogenetic inhibition of BLA^{Glu} terminals in the mPFC of mice treated with quinpirole 15 times (n = 5 to 7 mice per group, frequency: $F_{1,10}$ = 14.88, P = 0.003; drink time: $F_{1,10}$ = 5.48, P = 0.04). (*L*) Schematic of viral injection. (*M* and *N*) OCD-like behavioral effects of optogenetic activation of BLA^{Glu} terminals in the mPFC of mice treated with quinpirole seven times (n = 5 mice per group, frequency: $F_{1,8}$ = 27.13, P < 0.001; drink time: $F_{1,8}$ = 6.45, P = 0.035). Data are means ± SEM. *P < 0.05, **P < 0.01, ***P < 0.001. Two-way repeated-measures ANOVA with Bonferroni post hoc analysis for *E*; unpaired t test for *H*; one-way ANOVA with Bonferroni post hoc analysis for *J*, *K*, *M*, and *N*.

of saline mice (Fig. 4 *D* and *E*). Using in vivo microdialysis-HPLC, we found that the concentration of glutamate in the mPFC was increased in the quinpirole mice (35.07 ± 9.03 μM) relative to saline mice (3.59 ± 1.54 μM, Fig. 4 *F–H* and *SI Appendix*, Fig. S7). These results suggest an increase in BLA^{Glu}–mPFC-projecting neuronal activity in OCD states. In contrast, this difference was not obtained on days 6, 10, and 14 after quinpirole treatment (*SI Appendix*, Fig. S8) or after 30-d chronic quinpirole treatment without environmental training (*SI Appendix*, Fig. S9). Consistent with these results, the BLA^{Glu} neuronal activity was also unchanged in naïve mouse brain slices by perfusion of quinpirole (*SI Appendix*, Fig. S10), indicating that the increased BLA^{Glu} neuronal activity is not likely attributable to the direct actions of quinpirole itself under OCD conditions.

To determine the role of the BLA^{Glu}→mPFC pathway in OCD-like checking behavior, we infused a *Cre*-dependent AAV carrying NpHR3.0 (AAV-DIO-eNpHR3.0-eYFP) into the BLA to suppress the activity of BLA^{Glu} axon projections in *CaMKII-Cre* mice (Fig. 4*I* and *SI Appendix*, Fig. S11 *A–C*). Optical stimulation in the mPFC restored the checking behaviors induced by quinpirole (Fig. 4 *J* and *K*). In addition, optical activation of BLA^{Glu} terminals in the mPFC accelerated the process of the quinpirole-induced routine of sucrose drinking (Fig. 4 *L–N* and *SI Appendix*, Fig. S11 *D–F*). These behavioral consequences established the functional causality of the BLA^{Glu}→mPFC pathway in the development of OCD-like checking behaviors.

The mPFC$^{GABA→Glu}$ Microcircuit for OCD-Like Checking Behavior. Given the enhanced BLA^{Glu}→mPFC input in checking behavior, we next investigated mPFC neuronal activity through whole-cell recordings performed in visualized glutamate and GABA neurons in brain slices. To visualize glutamate and GABA neurons, *CaMKII-Cre* mice and *GAD2-Cre* mice were crossed with *Ai14* (RCL-tdT) mice to produce transgenic mice with red tdTomato-expressing glutamate (*CaMKII-tdTOM*) or GABA (*GAD2-tdTOM*) neurons (Fig. 5 *A–H*). In the mPFC of quinpirole mice, the glutamate neuronal activity was decreased (Fig. 5 *A–C*), and the miniature IPSC frequency, but not amplitude, of mPFC^{Glu} neurons was

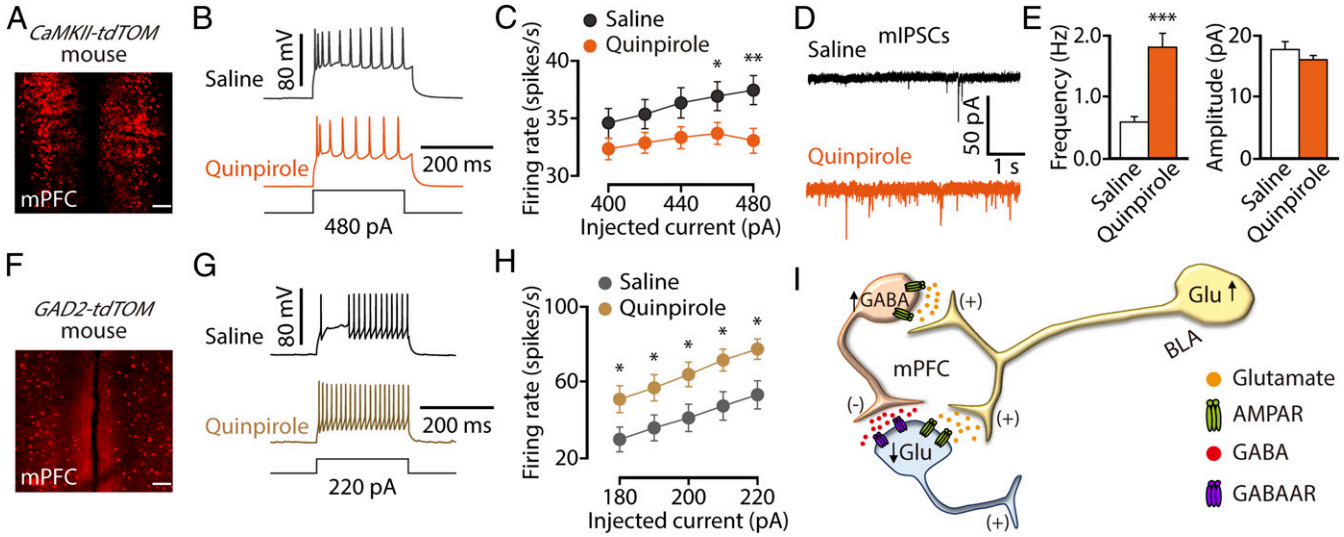

Fig. 5. Increased excitability of mPFC^{GABA} neurons inhibits mPFC^{Glu} neurons in OCD mice. (*A*) Sample image of the mPFC neurons in a *CaMKII-tdTOM* mouse. (Scale bar: 50 μm.) (*B* and *C*) Representative traces (*B*) and summarized data (*C*) of action potentials recorded from tdTOM$^+$ neurons in the mPFC slices from mice treated with quinpirole or saline for 30 d (n = 23 to 26 neurons per group, $F_{1,47}$ = 4.16, P = 0.047). (*D*) Representative traces of miniature IPSCs (mIPSCs) from tdTOM$^+$ neurons in the mPFC of mice treated with quinpirole or saline for 30 d. (*E*) Summarized data of the frequency and amplitude of mIPSCs from the groups in *D* (n = 20 to 22 neurons per group, frequency: t_{40} = −5.30, P < 0.001; amplitude: t_{40} = 1.16, P = 0.25). (*F*) Sample image of the mPFC neurons in a *GAD2-tdTOM* mouse. (Scale bar: 50 μm.) (*G* and *H*) Representative traces (*G*) and summarized data (*H*) of action potentials recorded from mPFC tdTOM$^+$ neurons of mice treated with quinpirole or saline for 30 d (n = 25 to 28 neurons per group, $F_{1,51}$ = 5.84, P = 0.019). (*I*) A model of feedforward inhibition BLA^{Glu}→mPFC$^{GABA→Glu}$ circuits in OCD-like checking behavior. Data are means ± SEM. *P < 0.05, **P < 0.01, ***P < 0.001. Two-way repeated-measures ANOVA with Bonferroni post hoc analysis for *C* and *H*; unpaired t test for *E*. AMPAR, AMPA receptor; GABAAR, GABA$_A$ receptor.

increased (Fig. 5 *D* and *E*). In contrast, the GABA neuronal activity was increased (Fig. 5 *F*–*H*). These results suggest that the enhanced BLA^{Glu} input to mPFC^{GABA} drives more effective inhibition of mPFC^{Glu} neurons (Fig. 5*I*), which is supported by the model of BLA–mPFC GABA feedforward inhibition (18, 19, 29).

We subsequently investigated whether inhibition of mPFC^{GABA} neurons or activation of mPFC^{Glu} neurons could restore the OCD-like checking behavior. Using *Cre*-dependent expression of the chemogenetic inhibitory hM4Di in the mPFC and i.p. injection of its ligand (clozapine-*N*-oxide) to selectively inhibit mPFC^{GABA} neurons in *GAD2-Cre* mice treated with quinpirole (Fig. 6*A* and *SI Appendix*, Fig. S12*A*), the sucrose-drinking behavior pattern was reversed (Fig. 6 *B* and *C*). A similar result was obtained using hM3Dq to activate mPFC^{Glu} neurons in *CaMKII-Cre* mice treated with quinpirole (Fig. 6 *D* and *E* and *SI Appendix*, Fig. S12*B*). In addition, chemogenetic inhibition of mPFC^{Glu} or activation of mPFC^{GABA} neurons significantly accelerated the process of quinpirole-induced checking behaviors (*SI Appendix*, Fig. S12 *C*–*I*). These results demonstrate that the BLA^{Glu}→mPFC$^{GABA→Glu}$ circuit is, at least in part, an inhibitory circuit that governs OCD-like checking behavior.

Discussion

In this work, we established an OCD mouse model in the form of quinpirole-induced checking routines accompanied by anxiety, which is analogous to the pathological behavior of OCD checkers. Complementary to the quinpirole model in rats (22), this study established OCD-like checking behavior in mice by pharmacological manipulations. Specifically, mice reliably and relatively rapidly formed OCD-like behavior and maintained it for at least 21 d in the study environment. Unlike transgenic strains (30–32) and optogenetic manipulations billed as animal models of OCD characterized by excessively self-destructive grooming behavior (7, 8, 33), our mouse model is beneficial

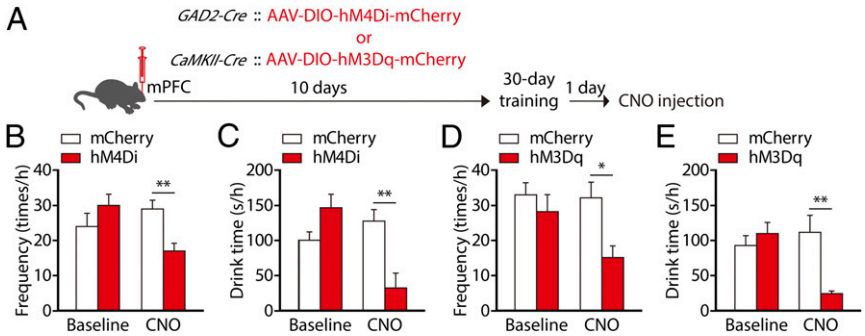

Fig. 6. The mPFC$^{GABA→Glu}$ microcircuit controls OCD-like checking behavior. (*A*) Experimental timeline for chemogenetic manipulations. (*B*–*E*) OCD-like behavioral effects of chemogenetic inhibition of mPFC^{GABA} neurons in *GAD2-Cre* mice (*B* and *C*, n = 5 mice per group, frequency: $F_{1,8}$ = 12.86, P = 0.007; drink time: $F_{1,8}$ = 12.75, P = 0.007) or chemogenetic activation of mPFC^{Glu} neurons in *CaMKII-Cre* mice treated with quinpirole (*D* and *E*, n = 6 mice per group, frequency: $F_{1,10}$ = 9.40, P = 0.012; drink time: $F_{1,10}$ = 12.49, P = 0.005). Data are means ± SEM. *P < 0.05, **P < 0.01. One-way ANOVA with Bonferroni post hoc analysis for *B*–*E*. CNO, clozapine-*N*-oxide.

for the exploration of the mechanisms underlying the process of OCD-associated checking phenotypes.

Different OCD symptoms may require distinct neural circuits (10, 34). Due to the inherently limited ability to study the neural substrates of OCD in humans, the precise mechanism underlying these symptoms remains elusive. The advantage of studying the neural circuit mechanism of a disorder is that it can reveal the convergent pathologically behavioral consequences. In this study, we propose a hypothesis for the neural circuit mechanism of checking symptoms in an OCD mouse model. Central to this process is the excitation of BLA^{Glu} neurons projecting to both $mPFC^{GABA}$ and $mPFC^{Glu}$ neurons. A decrease in this circuit activity is caused by inhibition of $mPFC^{Glu}$ neurons by $mPFC^{GABA}$ local interneurons via receiving enhanced BLA^{Glu} inputs. In particular, our results showed that environment-induced adaptations of this circuit drive OCD-like checking symptoms. These findings suggest that the $BLA^{Glu}\rightarrow mPFC^{GABA\rightarrow Glu}$ circuit could be an upstream input to the CSTC circuitry, which is an essential complementary part of the BLA–CSTC model in the pathophysiology of OCD. Although the most accurate way to segregate OCD into different subtypes is still a matter of active investigation and debate, the $BLA^{Glu}\rightarrow mPFC^{GABA\rightarrow Glu}$ circuit may contribute to the development or maintenance of checking compulsions.

Previous studies have reported the dopaminergic regulation of transmission in the BLA–mPFC pathway of distinct executive functions in vivo (35). In the current study, we dissected the precise organization of the $BLA^{Glu}\rightarrow mPFC^{GABA\rightarrow Glu}$ circuit by using a broad range of methodologies. Importantly, although this pathway likely contributes to multiple ongoing behavioral actions such as anxiety, fear acquisition, expression, and extinction (18–20), we elucidated a functional link between this circuit and the OCD-like checking symptoms. This finding is supported by a previous study showing that cognitive behavioral therapy (CBT) decreases BLA–ventromedial PFC connectivity, which predicts a better CBT outcome in patients with OCD (27). It is reasonable to suppose that certain neurocircuitry in the brain controls multiple behavioral responses, including OCD.

In summary, this study defines a critical $BLA^{Glu}\rightarrow mPFC^{GABA\rightarrow Glu}$ circuit through which compulsive checking behavior is generated. A mechanistic functional understating of this circuit will provide insight into the possible mechanisms underlying human OCD checking symptoms.

Materials and Methods

See *SI Appendix, Materials and Methods* for additional detailed information about the procedures used in this study. All data necessary to understand and assess the conclusions of this study are available in the main text or in *SI Appendix*. There are no restrictions on data availability in the manuscript.

Animals. Male mice at 8 to 10 wk of age were used. All animal protocols were approved by the Animal Care and Use Committee of the University of Science and Technology of China.

Animal Model of Compulsive Sucrose Drinking Behavior. Chronic injection of quinpirole hydrochloride (0.75 mg/kg) was used to construct an OCD-like behavioral mouse model.

Brain Slice Preparation. Acute brain slices were prepared as previously described (36).

Statistical Analysis. The Student's *t* test or ANOVA was used. All data are expressed as the mean ± SEM.

ACKNOWLEDGMENTS. We thank the Center for Advanced Imaging at the Institute of Automation of the Chinese Academy of Sciences for the fMRI experiments in mice. This work was supported by grants from the National Natural Science Foundation of China (91732303, 31600851, 81600964, and 81870877), the National Key Research and Development Program of China (2016YFC1305900), and the Strategic Priority Research Program of the Chinese Academy of Sciences (XDB02010000).

1. Ridley RM (1994) The psychology of perserverative and stereotyped behaviour. *Prog Neurobiol* 44:221–231.
2. Kessler RC, et al. (2005) Lifetime prevalence and age-of-onset distributions of DSM-IV disorders in the National Comorbidity Survey Replication. *Arch Gen Psychiatry* 62: 593–602, and erratum (2005) 62:768.
3. Kalueff AV, et al. (2016) Neurobiology of rodent self-grooming and its value for translational neuroscience. *Nat Rev Neurosci* 17:45–59.
4. Franklin ME, Foa EB (2011) Treatment of obsessive compulsive disorder. *Annu Rev Clin Psychol* 7:229–243.
5. Saxena S, Rauch SL (2000) Functional neuroimaging and the neuroanatomy of obsessive-compulsive disorder. *Psychiatr Clin North Am* 23:563–586.
6. Chamberlain SR, et al. (2008) Orbitofrontal dysfunction in patients with obsessive-compulsive disorder and their unaffected relatives. *Science* 321:421–422.
7. Ahmari SE, et al. (2013) Repeated cortico-striatal stimulation generates persistent OCD-like behavior. *Science* 340:1234–1239.
8. Burguière E, Monteiro P, Feng G, Graybiel AM (2013) Optogenetic stimulation of lateral orbitofronto-striatal pathway suppresses compulsive behaviors. *Science* 340:1243–1246.
9. Pauls DL, Abramovitch A, Rauch SL, Geller DA (2014) Obsessive-compulsive disorder: An integrative genetic and neurobiological perspective. *Nat Rev Neurosci* 15:410–424.
10. Mataix-Cols D, et al. (2004) Distinct neural correlates of washing, checking, and hoarding symptom dimensions in obsessive-compulsive disorder. *Arch Gen Psychiatry* 61:564–576.
11. Nagai M, Kishi K, Kato S (2007) Insular cortex and neuropsychiatric disorders: A review of recent literature. *Eur Psychiatry* 22:387–394.
12. Milad MR, Rauch SL (2012) Obsessive-compulsive disorder: Beyond segregated cortico-striatal pathways. *Trends Cogn Sci* 16:43–51.
13. Häge A, et al.; TACTICS Consortium (2016) Glutamatergic medication in the treatment of obsessive compulsive disorder (OCD) and autism spectrum disorder (ASD)–Study protocol for a randomised controlled trial. *Trials* 17:141.
14. Chakrabarty K, Bhattacharyya S, Christopher R, Khanna S (2005) Glutamatergic dysfunction in OCD. *Neuropsychopharmacology* 30:1735–1740.
15. Janak PH, Tye KM (2015) From circuits to behaviour in the amygdala. *Nature* 517:284–292.
16. Simon D, Adler N, Kaufmann C, Kathmann N (2014) Amygdala hyperactivation during symptom provocation in obsessive-compulsive disorder and its modulation by distraction. *Neuroimage Clin* 4:549–557.
17. Szeszko PR, et al. (2004) Amygdala volume reductions in pediatric patients with obsessive-compulsive disorder treated with paroxetine: Preliminary findings. *Neuropsychopharmacology* 29:826–832.
18. Felix-Ortiz AC, Burgos-Robles A, Bhagat ND, Leppla CA, Tye KM (2016) Bidirectional modulation of anxiety-related and social behaviors by amygdala projections to the medial prefrontal cortex. *Neuroscience* 321:197–209.
19. Klavir O, Prigge M, Sarel A, Paz R, Yizhar O (2017) Manipulating fear associations via optogenetic modulation of amygdala inputs to prefrontal cortex. *Nat Neurosci* 20:836–844.
20. Burgos-Robles A, et al. (2017) Amygdala inputs to prefrontal cortex guide behavior amid conflicting cues of reward and punishment. *Nat Neurosci* 20:824–835.
21. Carlsen J (1988) Immunocytochemical localization of glutamate decarboxylase in the rat basolateral amygdaloid nucleus, with special reference to GABAergic innervation of amygdalostriatal projection neurons. *J Comp Neurol* 273:513–526.
22. Szechtman H, Sulis W, Eilam D (1998) Quinpirole induces compulsive checking behavior in rats: A potential animal model of obsessive-compulsive disorder (OCD). *Behav Neurosci* 112:1475–1485.
23. Amato D, Milella MS, Badiani A, Nencini P (2006) Compulsive-like effects of repeated administration of quinpirole on drinking behavior in rats. *Behav Brain Res* 172:1–13.
24. Eilam D (2017) From an animal model to human patients: An example of a translational study on obsessive compulsive disorder (OCD). *Neurosci Biobehav Rev* 76:67–76.
25. Hoffman GE, Smith MS, Verbalis JG (1993) c-Fos and related immediate early gene products as markers of activity in neuroendocrine systems. *Front Neuroendocrinol* 14:173–213.
26. Phillips ML, et al. (2000) A differential neural response in obsessive-compulsive disorder patients with washing compared with checking symptoms to disgust. *Psychol Med* 30:1037–1050.
27. Fullana MA, et al. (2017) Basolateral amygdala-ventromedial prefrontal cortex connectivity predicts cognitive behavioural therapy outcome in adults with obsessive-compulsive disorder. *J Psychiatry Neurosci* 42:378–385.
28. Wickersham IR, et al. (2007) Monosynaptic restriction of transsynaptic tracing from single, genetically targeted neurons. *Neuron* 53:639–647.
29. McGarry LM, Carter AG (2016) Inhibitory gating of basolateral amygdala inputs to the prefrontal cortex. *J Neurosci* 36:9391–9406.
30. Shmelkov SV, et al. (2010) Slitrk5 deficiency impairs corticostriatal circuitry and leads to obsessive-compulsive-like behaviors in mice. *Nat Med* 16:598–602.
31. Welch JM, et al. (2007) Cortico-striatal synaptic defects and OCD-like behaviours in Sapap3-mutant mice. *Nature* 448:894–900.
32. Ting JT, Feng G (2011) Neurobiology of obsessive-compulsive disorder: Insights into neural circuitry dysfunction through mouse genetics. *Curr Opin Neurobiol* 21:842–848.
33. Szechtman H, et al. (2016) Obsessive-compulsive disorder: Insights from animal models. *Neurosci Biobehav Rev* 76:254–279.
34. van den Heuvel OA, et al. (2009) The major symptom dimensions of obsessive-compulsive disorder are mediated by partially distinct neural systems. *Brain* 132:853–868.
35. Floresco SB, Tse MT (2007) Dopaminergic regulation of inhibitory and excitatory transmission in the basolateral amygdala-prefrontal cortical pathway. *J Neurosci* 27: 2045–2057.
36. Zhang Z, Cai YQ, Zou F, Bie B, Pan ZZ (2011) Epigenetic suppression of GAD65 expression mediates persistent pain. *Nat Med* 17:1448–1455.